

A Lyman- α Galaxy at Redshift $z = 6.944$ in the COSMOS Field¹

James E. Rhoads¹, Pascale Hibon^{1,2}, Sangeeta Malhotra¹, Michael Cooper^{3,4}, Benjamin Weiner⁵

ABSTRACT

Lyman- α emitting galaxies can be used to study cosmological reionization, because a neutral intergalactic medium scatters Lyman- α photons into diffuse halos whose surface brightness falls below typical survey detection limits. Here we present the Lyman- α emitting galaxy LAE J095950.99+021219.1, identified at redshift $z = 6.944$ in the COSMOS field using narrowband imaging and followup spectroscopy with the IMACS instrument on the Magellan I Baade telescope. With a single object spectroscopically confirmed so far, our survey remains consistent with a wide range of IGM neutral fraction at $z \approx 7$, but further observations are planned and will help clarify the situation. Meantime, the object we present here is only the third Lyman- α -selected galaxy to be spectroscopically confirmed at $z \gtrsim 7$, and is ~ 2 – 3 times fainter than the previously confirmed $z \approx 7$ Lyman- α galaxies.

Subject headings: galaxies: high-redshift — dark ages, reionization, first stars

1. Introduction

Lyman- α emitting galaxies provide a valuable probe of reionization, because resonant scattering of Lyman- α photons in the intergalactic medium (IGM) can suppress the observed

¹School of Earth and Space Exploration, Arizona State University, Tempe, AZ 85287; email malhotra@asu.edu, James.Rhoads@asu.edu

²Gemini Observatory, La Serena, Chile; email phibon@gemini.edu

³Center for Galaxy Evolution, Department of Physics and Astronomy, University of California, Irvine, 4129 Frederick Reines Hall, Irvine, CA 92697, USA; m.cooper@uci.edu

⁴Hubble Fellow

⁵Steward Observatory, University of Arizona

¹This paper includes data gathered with the 6.5 meter Magellan Telescopes located at Las Campanas Observatory, Chile

Lyman- α line by a factor of $\gtrsim 3$ for any neutral fraction $\gtrsim 50\%$ (Malhotra & Rhoads 2004; Santos 2004). Such strong flux suppression will cause a change in the Lyman- α luminosity function that should be obvious— especially since Lyman- α galaxies show little evolution at $3 \lesssim z \lesssim 6$, either in luminosity function (Dawson et al. 2007; Zheng et al. 2012) or physical properties (Malhotra et al. 2012). Early studies concluded that the IGM neutral fraction was already small at $z \approx 6.5$ (Malhotra & Rhoads 2004; Stern et al. 2005). More recent work has established the Lyman- α luminosity function at both $z \approx 5.7$ and 6.5 to considerable accuracy (Ouchi et al. 2010; Hu et al. 2010; Kashikawa et al. 2011), showing a modest but statistically significant difference between these observed Lyman- α luminosity functions: The $z = 6.5$ luminosity function is below that at $z = 5.7$, and the difference can be adequately characterized by a pure luminosity evolution by a factor of ~ 1.3 (Ouchi et al. 2010).

Yet, other Lyman- α based tests for reionization— including the apparent spatial clustering of Lyman- α galaxies (McQuinn et al. 2007), the minimum ionized volume around observed Lyman- α sources (Malhotra & Rhoads 2006), and Lyman- α line profiles (Hu et al. 2010; Ouchi et al. 2010)— show little evidence for neutral gas at $z \approx 6.5$. This leaves an open question— is lower Lyman- α luminosity function at $z = 6.5$ due to neutral gas, or is it an intrinsic evolution in the galaxy populations?

To distinguish between these possibilities, we can look to still higher redshifts, where the IGM neutral fraction should be higher and its effects on Lyman- α stronger. The highest redshift readily accessible to Lyman- α searches using CCDs is $z \approx 7.0$, in the 9650Å window in the night sky OH emission spectrum. We are pursuing a 9650Å narrowband survey using the IMACS imaging spectrograph on the 6.5m Magellan I Baade Telescope at Las Campanas Observatory (Hibon et al. 2011). We surveyed 465 square arcminutes, corresponding to $\sim 72000\text{Mpc}^3$. After a careful selection, we found 6 $z \sim 6.96$ LAE candidates (Hibon et al. 2011). To confirm whether these are real LAEs, we obtained multi-object spectra with IMACS. In this *Letter*, we present the spectrum of LAE J095950.99+021219.1, which was identified as a candidate redshift $z \approx 7$ Lyman- α emitting galaxy (candidate LAE 3) in Hibon et al. (2011). Our spectroscopy reveals a single, isolated Lyman- α line at redshift $z = 6.944$.

Throughout the paper, we adopt a Λ CDM “concordance cosmology” with $\Omega_M = 0.27$, $\Omega_\Lambda = 0.73$, and $H_0 = 71 \text{ km s}^{-1} \text{ Mpc}^{-1}$.

2. Spectroscopic Observations and Analysis

2.1. Observations

We observed our candidate $z \approx 7$ Lyman- α galaxies using the Inamori Magellan Areal Camera and Spectrograph (IMACS) on the 6.5m Magellan I Baade Telescope on the nights of 29–30 December 2010, and 8 February 2011. The February data were of lower quality and are not used here. We used custom multi-slit masks, shared between two primary observing programs. We selected the f/2 camera and the 300-line red-blazed grism with 1" slitlets as the best compromise between areal coverage, spectral coverage, and spectral resolution.

Observations were split among five slit masks (two per night in December, and one in February). The time per mask and observing conditions are summarized in table 1. While the position angle of the masks were not all identical, the data were taken without dithering the telescope. Moreover, the targets were centered on their slitlets, and LAE J095950.99+021219.1 is compact compared to the seeing. This allows us to combine all of the spectroscopic data into a single 1D spectrum (see below).

2.2. Data Reduction

We performed initial data reduction steps using the COSMOS software package². COSMOS steps include bias frame subtraction, spectroscopic flat fielding using continuum (quartz) lamp exposures, and wavelength calibration using arc lamp exposures. COSMOS also sky-subtracts the spectra, using the Kelson (2003) algorithm to remove night sky lines. Finally, COSMOS extracts a 2D, rectified spectrum for each slitlet.

²Note the double meaning of the acronym COSMOS. We deny any responsibility for the ensuing confusion.

Mask ID	Observation date (UT)	Number of exposures	Time per exposure	Seeing (approx)
COSMOS1	30 Dec 2010	4	1800	0.5–0.9"
COSMOS2	30 Dec 2010	3	1800	0.5–0.9"
COSMOS3	31 Dec 2010	4	1800	1–1.5"
COSMOS4	31 Dec 2010	3	1860	1–1.5"
COSMOS-Feb	8 Feb 2011	5	1800	1.2–2"

Table 1: Summary of slit mask observations.

We performed subsequent steps in two ways, either (a) combining exposures from each mask separately, and then combining results from different masks; or (b) directly combining all exposures from multiple masks.

Treating masks separately gives four 2D spectra of LAE J095950.99+021219.1 from December, and one more from February. Most of these 2D stacks show a weak but visible emission line in the spectrum of LAE J095950.99+021219.1. We next combined the four December spectra into a stacked 2D spectrum comprising our best 7.05 hours of data. To do this, we first averaged the four 2D spectra. Next, we made a median-combined stack. We then subtracted the two, and computed the (sigma-clipped) noise level in the difference. Finally, we constructed a hybrid stack, using the value from the average stack almost everywhere, but the value from the median stack wherever the difference between these two stacks exceeded 10σ . This yields a lower noise estimate than the median, yet remains more robust to outliers than the mean. The emission line becomes readily evident in this combined stack.

To test the robustness of our results, we also combined all December exposures in single 14-frame stacks, using various outlier rejection schemes (median stacking with 3- and 5σ rejection, and average stacking with 2.5σ rejection). The emission line remains comparably significant in all of these stacks. The stacked 2D spectrum around the emission line, using average stacking and 2.5σ rejection, is shown in figure 1.

We also made stacks by bootstrap resampling, stacking 14 exposures selected randomly with repetitions permitted. We remeasured the flux at the location of the detected line, using aperture photometry in the 2D stacks. The bootstrap fluxes were $104\% \pm 10\%$ of the “normal” stack flux for a 10-pixel diameter ($2'' \times 20\text{\AA}$) aperture, and $116\% \pm 21\%$ for a 14-pixel diameter ($2.8'' \times 28\text{\AA}$) aperture. Among 1000 bootstrap simulations, the lowest measured fluxes were 77% and 66% of “normal” for the 10- and 14-pixel apertures. The observed line is therefore not a fluke caused by a handful of exposures.

We next extracted a 1D spectrum from the two-stage stacking (method “a”), using the IRAF task “apall” with an unweighted extraction of $1.4''$ (7 pixel) window width, centered on the emission line and parallel to the dispersion axis. (COSMOS 2D output has the dispersion axis parallel to the x -axis, so we need not fit a trace to the continuum, which is undetected in the present data anyway.) We performed no further sky subtraction, since that too is done by the COSMOS package. To get another estimate of the noise level in the data, we extracted five further 1D spectra from the 2D stacked spectrum, each at a different spatial position along the slit. Each should be essentially a pure noise spectrum. The variance among these five parallel traces provides a wavelength-dependent noise estimate, and the line is significant at the 4.5σ level against this estimate. The extracted 1D spectrum is shown in figure 2.

Significance: To explore the significance of the line detection, we measured aperture fluxes at a grid of clean locations in the 2D spectrum of LAE J095950.99+021219.1 (after rescaling the 2D spectrum by the noise ratio $\sigma(9658\text{\AA})/\sigma(\lambda)$). The RMS counts among these apertures corresponds to a 1σ noise of $1.34 \times 10^{-18} \text{ erg cm}^{-2} \text{ s}^{-1}$, against which our line is a 6.3σ event. Among $\gtrsim 400$ non-overlapping 5-pixel apertures, the brightest two were 4.1σ and 3.2σ events (65% and 51% as bright as the LAE J095950.99+021219.1 line), suggesting only mildly non-gaussian noise.

The search that found this line was based on 6 candidates, each with a position known to $1''$ and an expected line wavelength known to $\Delta\lambda = 90\text{\AA}$. Given our spatial and spectral resolution, this corresponds to $\sim 6 \times 2 \times 20 = 240$ independent resolution elements. Our significance level estimates range from 4.5σ to 6.3σ , and for Gaussian noise, the corresponding chance probabilities in 240 trials range from $< 10^{-3}$ to $< 10^{-7}$.

Spectroscopic flux calibration: Each mask included two blue stars with well measured photometry from the COSMOS project (Capak et al. 2007). We flux calibrate the observed emission line of LAE J095950.99+021219.1 by direct comparison with the observed counts in one of these stars, which was observed under identical conditions as our science targets. Both the emission line count rate and the comparison star’s count rate per unit wavelength were measured directly in the 2D spectra and at the same wavelength. For the emission line, we used the 10-pixel diameter ($2'' \times 20\text{\AA}$) aperture. This yields a flux of $8.5 \times 10^{-18} \text{ erg cm}^{-2} \text{ s}^{-1}$ for LAE J095950.99+021219.1, corresponding to line luminosity $4.9 \times 10^{42} \text{ erg s}^{-1}$ at $z = 6.944$.

The fractional uncertainties in this flux are $\sim 20\%$ from photon counting statistics (with a statistical signal-to-noise ratio of $s/n = 4.5\text{--}6.3$ from the 1D or 2D spectra), 12% from the choice of aperture used to measure the line flux in the 2D spectrum, and $\leq 10\%$ from the assumption that the comparison star’s flux density at 9680\AA equals its z -band flux density. The final spectroscopic flux measurement is $(8.5 \pm 2) \times 10^{-18} \text{ erg cm}^{-2} \text{ s}^{-1}$.

2.3. Comparison to narrowband imaging results:

The observed spectroscopic line flux is smaller than the narrowband flux (Hibon et al. 2011). Part of the discrepancy can be attributed to continuum in the narrowband filter. The emission line is near the blue edge of the filter bandpass, so continuum emission redward of the line will contribute relatively strongly to the narrow band flux.

We also re-examined the narrowband flux measurements for LAE J095950.99+021219.1.

Following Hibon et al. (2011), we used moderately bright stars that are well detected but unsaturated in both the public COSMOS z -band image and our NB9680 image. The narrowband magnitudes in Hibon et al. (2011) were based on $1''$ diameter aperture fluxes, with an aperture correction based on the difference between SExtractor “magiso” and aperture fluxes (see Hibon et al. (2011) for more details). In the present work, we omitted the aperture correction step, using instead identical $1.2''$ diameter flux measurements for both the science objects and the reference stars in the NB9680 image. (The precise aperture diameter is unimportant, since LAE J095950.99+021219.1 is compact compared to the point spread function.) We obtained a narrowband magnitude $NB9680_{AB} = 24.86 \pm 0.18$. The corresponding narrowband flux is $12 \times 10^{-18} \text{ erg cm}^{-2} \text{ s}^{-1}$.

This is almost 50% more than the spectroscopically determined emission line flux (a 1.5σ difference). If we attribute the difference to continuum emission in the narrowband filter, the corresponding flux density is $f_\lambda \sim (f_{NB} - f_{spec})/\Delta\lambda \approx 3.5 \times 10^{-18}/60\text{\AA} \approx 5.8 \times 10^{-20} \text{ erg cm}^{-2} \text{ s}^{-1} \text{ \AA}^{-1}$, or $AB = 25.75$. The implied observer-frame equivalent width is $\sim 120\text{\AA}$ (though consistent with an arbitrarily large equivalent width at 1.5σ). While the object is undetected in the z' filter down to $AB > 26.4$, a continuum magnitude of 25.75 *redward of the line at 9657\AA* remains allowed, since most of the z' filter’s transmission lies blueward of that wavelength. The object is also undetected in the WIRDS J-band image (Bielby & al 2012, in prep), with a $1.2''$ aperture flux $\sim (1.8 \pm 2.1) \times 10^{-30} \text{ erg cm}^{-2} \text{ s}^{-1} \text{ Hz}^{-1}$, corresponding to $J_{AB} \gtrsim 24.1$ (3σ).

3. Interpretation

We interpret the line at 9657\AA in LAE J095950.99+021219.1 as Lyman- α at redshift $z = 6.944$, based on non-detections in all filters blueward of this line, and on the absence of other optical lines.

Were the primary line $H\alpha$ (at $z \approx 0.472$), or [O III] $\lambda 5007$ (at $z \approx 0.928$), we would expect other prominent emission lines in our IMACS spectrum. Figure 3 shows non-detections in the 1D spectrum at the expected line wavelengths. Corresponding upper limits are summarized in table 2. The “ $H\alpha$ ” case ($z \approx 0.472$) is disfavored by the non-detections of [O III] $\lambda 5007$ and [O II] $\lambda 3727$, with 3σ line ratio limits $f(\text{O III})/f(H\alpha) < 1/2$ and $f(\text{O II})/f(H\alpha) < 2/3$. If the primary line is [O III] $\lambda 5007$, unfortunately placed night-sky line residuals overlap the expected locations of [O III] $\lambda 4959$ and $H\beta$, precluding interesting limits. Fortunately, the expected [O II] $\lambda 3727$ line location is clean, and gives a tight upper limit $f(\text{O II})/f(\text{O III}) < 0.2$ (3σ). This provides some evidence against the [O III] $\lambda 5007$ interpretation. Ratios of $f(\text{O II})/f(\text{O III})$ this small are seen in a significant minority of star

forming galaxies (Xu et al. 2007; McLinden et al. 2011; Richardson et al. 2011, in prep; Xia et al. 2012, in prep), but more can be ruled out by this line ratio.

To address the [O II] $\lambda 3727$ possibility and further improve our constraints on [O III] $\lambda 5007$, we examine equivalent widths. Following Hibon et al. (2011), we combine our spectroscopic line flux with optical magnitude limits of 27.9, 27.6, and 27.3 mag (5σ , AB) in g' , r' , and i' filters respectively. Since star-forming galaxies have $f_\nu \sim \text{constant}$, we have $f_\lambda(9657\text{\AA}) \approx 3.6 \times 10^{-20} \times 10^{-0.4 \times 28} \times c/(9657\text{\AA})^2 = 7.3 \times 10^{-21} \text{ erg cm}^{-2} \text{ s}^{-1} \text{ \AA}^{-1}$. The non-detection in these optical images then implies a 5σ limit $EW \equiv f_{\text{line}}/f_\lambda \approx (8 \times 10^{-18}/7.3 \times 10^{-21})\text{\AA} = 1100\text{\AA}$ (observer frame).

While [O III] $\lambda 5007$ and $H\alpha$ emission line sources with equivalent widths this large exist (Rhoads et al. 2000; Kakazu et al. 2007; Straughn et al. 2008, 2009; van der Wel et al. 2011; Atek et al. 2011), they are exceptional, rare objects. In Hibon et al. (2011), we estimated the numbers expected in our survey based on published line luminosity functions (Kakazu et al. 2007; Geach et al. 2010) and equivalent width distributions (Straughn et al. 2009). We found that $\lesssim 0.3$ [O III] $\lambda 5007$ emitters and $\lesssim 0.6$ $H\alpha$ emitters are expected.

[O II] $\lambda 3727$ emitters have generally smaller equivalent widths. We found *no* [O II] $\lambda 3727$ -selected objects with $EW \gtrsim 1100\text{\AA}/(1+z_{[OII]}) \approx 425\text{\AA}$ in the samples from Straughn et al. (2009) (30 objects), Kakazu et al. (2007) (24 objects), Xia et al. (2012, in prep) (11 objects), or Drozdovsky et al. (2005) (400 objects). Thus, $\lesssim 1/465 = 0.0022$ of [O II] $\lambda 3727$ emitters might enter our sample as LAE candidates. The luminosity function from Rigopoulou et al. (2005) suggests that our survey volume should contain ~ 45 [O II] $\lambda 3727$ galaxies. Among these, $\lesssim 0.1$ object should pass our Lyman- α selection criteria.

Thus, the aggregate sample of foreground emitters expected in our survey is < 1 galaxy. In contrast, our survey volume at $z \approx 6.95$ should contain between ~ 2.5 and ~ 11 Lyman- α galaxies with line fluxes $\gtrsim 8 \times 10^{-18} \text{ erg cm}^{-2} \text{ s}^{-1}$, based on the $z \approx 6.5$ luminosity functions of Hu et al. (2010) and Ouchi et al. (2010). We thus regard Lyman- α as the best interpretation of the observed emission line.

4. Discussion

Redshift $z \approx 7$ is the current frontier in reionization studies, an area of active exploration where our observational knowledge is growing rapidly.

The recently discovered quasar at $z \approx 7.1$ (Mortlock et al 2011), combined with spectroscopic followup (and occasional confirmation) of $z \sim 7$ galaxy candidates from HST WFC3

surveys, provide an unprecedented look at this epoch. Observations of these objects seem to favor the continued existence of significant neutral intergalactic gas as late as $z \sim 7$. This is surprising, given that microwave background polarization data from WMAP favor a characteristic reionization redshift $z_r \sim 11$, and that the IGM at $z \sim 6.2$ is highly ionized, with a neutral fraction of only 1–4% based on quasar spectra (Fan et al 2006). Nonetheless, the ionized bubble around the $z \approx 7.1$ quasar appears too small to be comfortably explained in a fully ionized medium, unless the quasar is itself remarkably young ($\sim 10^6$ years) (Bolton et al 2011). Similarly, three independent research groups have argued that the fraction of $z \sim 7$ Lyman break candidates showing Lyman- α emission appears smaller than would be expected in an ionized medium (Vanzella et al 2010; Stark et al 2010; Ono et al 2011; Schenker et al 2011; Pentericci et al 2011). Still, these results depend on the reliability of photometric selection criteria, and a contamination of order 50% could explain the observations without recourse to neutral gas (e.g., Schenker et al 2011).

Lyman- α galaxy surveys offer a complementary approach to studying reionization. The underlying physics is the same as for spectroscopic followup of Lyman break samples, but the survey selection proceeds differently, leading to different potential selection biases. The uncertainties in the method are likewise very different from those associated with the quasar near-zone measurement (Mortlock et al. 2011; Bolton et al. 2011), or the Gunn-Peterson trough (Fan et al. 2006). Because of this, conclusions about cosmological reionization will be strongest when they are based on multiple independent methods.

The work we present here is only the second large-area narrowband survey for Lyman- α galaxies at redshift $z \approx 7.0$, following on the work of Iye et al. (2006) and Ota et al. (2010). The spectroscopic confirmation of LAE J095950.99+021219.1 demonstrates that such objects can be identified at flux levels considerably fainter than the 2×10^{-17} erg cm $^{-2}$ s $^{-1}$ line of IOK-1 (Iye et al. 2006) or the recently reported $z \approx 7.2$ narrowband-selected Lyman- α galaxy SXDF-NB1006-2 (Shibuya et al. 2011). Our observed line flux, 8.5×10^{-18} erg cm $^{-2}$ s $^{-1}$, corresponds to a rest-frame line luminosity of only $L_{Ly\alpha} = (4.9 \pm 1) \times 10^{42}$ erg s $^{-1}$. This is at or below the characteristic line luminosity $L_{Ly\alpha}^*$ from Schechter function fits to $z \approx 6.5$ Lyman- α samples (e.g., $L_{Ly\alpha}^* = (4.4 \pm 0.6) \times 10^{42}$ erg s $^{-1}$ and $\Phi^* = 8.5 \times 10^{-4}$ cMpc $^{-3}$, Ouchi et al. (2010); $L_{Ly\alpha}^* = 1.0 \times 10^{43}$ erg s $^{-1}$ and $\Phi^* = 6 \times 10^{-5}$ cMpc $^{-3}$, Hu et al. (2010)).

Thus, our survey has achieved sensitivity to typical Lyman- α emitters. Were the $z = 7$ luminosity function unchanged from that at $z = 6.5$, we would expect our survey volume to contain 11 or 2.6 Lyman- α emitters brighter than LAE J095950.99+021219.1, based on the LF of Ouchi et al. (2010) or Hu et al. (2010) respectively. This reflects large differences in expectations from different published $z = 6.5$ luminosity functions. We will present a detailed analysis of our survey’s constraints on the Lyman- α luminosity function in a future

paper, after we have more sensitive spectra for our remaining candidates. For now, the galaxy LAE J095950.99+021219.1 is among the few most distant spectroscopically confirmed galaxies known, and the faintest to be discovered through a direct search for Lyman- α line emission.

JER, PH, and SM gratefully acknowledge support of the National Science Foundation through NSF grant AST-0808165. MCC acknowledges support from NASA through Hubble Fellowship grant #HF-51269.01-A, awarded by the Space Telescope Science Institute, which is operated by the Association of Universities for Research in Astronomy, Inc., for NASA, under contract NAS 5-26555; and from the Southern California Center for Galaxy Evolution, a multi-campus research program funded by the University of California Office of Research. We thank the staff of Las Campanas Observatory for their expert assistance throughout this project, and Gabriel Martin and David Osip in particular for their help with our filters. Finally, we thank the referee for a thorough and fair report.

REFERENCES

- Atek, H., et al. 2011, *ApJ* 743, 121
- Bielby, et al. 2012, submitted to *A&A*, arXiv:1111.6997
- Bolton, J. S., Haehnelt, M. G., Warren, S. J., Hewett, P. C., Mortlock, D. J., Venemans, B. P., McMahon, R. G., & Simpson, C. 2011, *MNRAS*, 416, L70
- Capak, P., et al. 2007, *ApJS*, 172, 99
- Dawson, S., Rhoads, J. E., Malhotra, S., Stern, E., Wang, J. X., Dey, A., Spinrad, H., & Jannuzi B. T. 2007, *ApJ* 671, 1227
- Drozdovsky, I., Yan, L., Chen, H.-W., Stern, D., Kennicutt, Jr., R., Spinrad, H., & Dawson, S. 2005, *AJ*, 130, 1324
- Fan, X., et al. 2006, *The Astronomical Journal*, 132, 117
- Geach, J. E., et al. 2010, *MNRAS*, 402, 1330
- Hibon, P., Malhotra, S., Rhoads, J., & Willott, C. J. 2011, *ApJ* 741, 101
- Hu, E. M., Cowie, L. L., Barger, A. J., Capak, P., Kakazu, Y., & Trouille, L. 2010, *ApJ*, 725, 394

- Iye, M., et al. 2006, *Nature*, 443, 186
- Kakazu, Y., Cowie, L. L., & Hu, E. M. 2007, *ApJ*, 668, 853
- Kashikawa, N., et al. 2011, *ApJ*, 734, 119
- Kelson, D. D. 2003, *PASP*, 115, 688
- Malhotra, S., & Rhoads, J. E. 2004, *ApJ*, 617, L5
- Malhotra, S., & Rhoads, J. E. 2004, *ApJ*, 617, L5
- . 2006, *ApJ*, 647, L95
- Malhotra, S., Rhoads, J. E., Finkelstein, S. L., Hathi, N., Nilsson, K., McLinden, E., & Pirzkal, N., *ApJ* 750, L36
- McLinden, E. M., et al. 2011, *ApJ*, 730, 136
- McQuinn, M., Hernquist, L., Zaldarriaga, M., & Dutta, S. 2007, *Monthly Notices of the Royal Astronomical Society*, 381, 75
- Mortlock, D. J., et al. 2011, *Nature*, 474, 616
- Ota, K., et al. 2010, *ApJ* 722, 803
- Ouchi, M., et al. 2010, *ApJ* 723, 869
- Rhoads, J. E., Malhotra, S., Dey, A., Stern, D., Spinrad, H., & Jannuzi, B. T. 2000, *ApJ*, 545, L85
- Richardson, M. L. A., McLinden, E. M., Malhotra, S., Rhoads, J. E., & Hibon, P. 2012, *ApJ*, in prep
- Rigopoulou, D., Vacca, W. D., Berta, S., Franceschini, A., & Aussel, H. 2005, *A&A*, 440, 61
- Santos, M. R. 2004, *Monthly Notices of the Royal Astronomical Society*, 349, 1137
- Shibuya, T., Kashikawa, N., Ota, K., Iye, M., Ouchi, M., Furusawa, H., Shimasaku, K. & Hattori, T., 2011, *ApJ*, submitted, arXiv:1112.3997v1
- Stern, D., Yost, S. A., Eckart, M. E., Harrison, F. A., Helfand, D. J., Djorgovski, S. G., Malhotra, S., & Rhoads, J. E. 2005, *ApJ*, 619, 12
- Straughn, A. N., et al. 2008, *The Astronomical Journal*, 135, 1624

—. 2009, *The Astronomical Journal*, 138, 1022

van der Wel, A., et al. 2011, *ApJ* 742, 111

Xia, L., et al. 2012, in prep

Xu, C., et al. 2007, *The Astronomical Journal*, 134, 169

Zheng, Z., Finkelstein, S. L., Finkelstein, K., Tilvi, V., Rhoads, J. E., Malhotra, S., Wang, J. X., Miller, N., Hibon, P., & Xia, L. 2011, arXiv:1111.3386, submitted to MNRAS

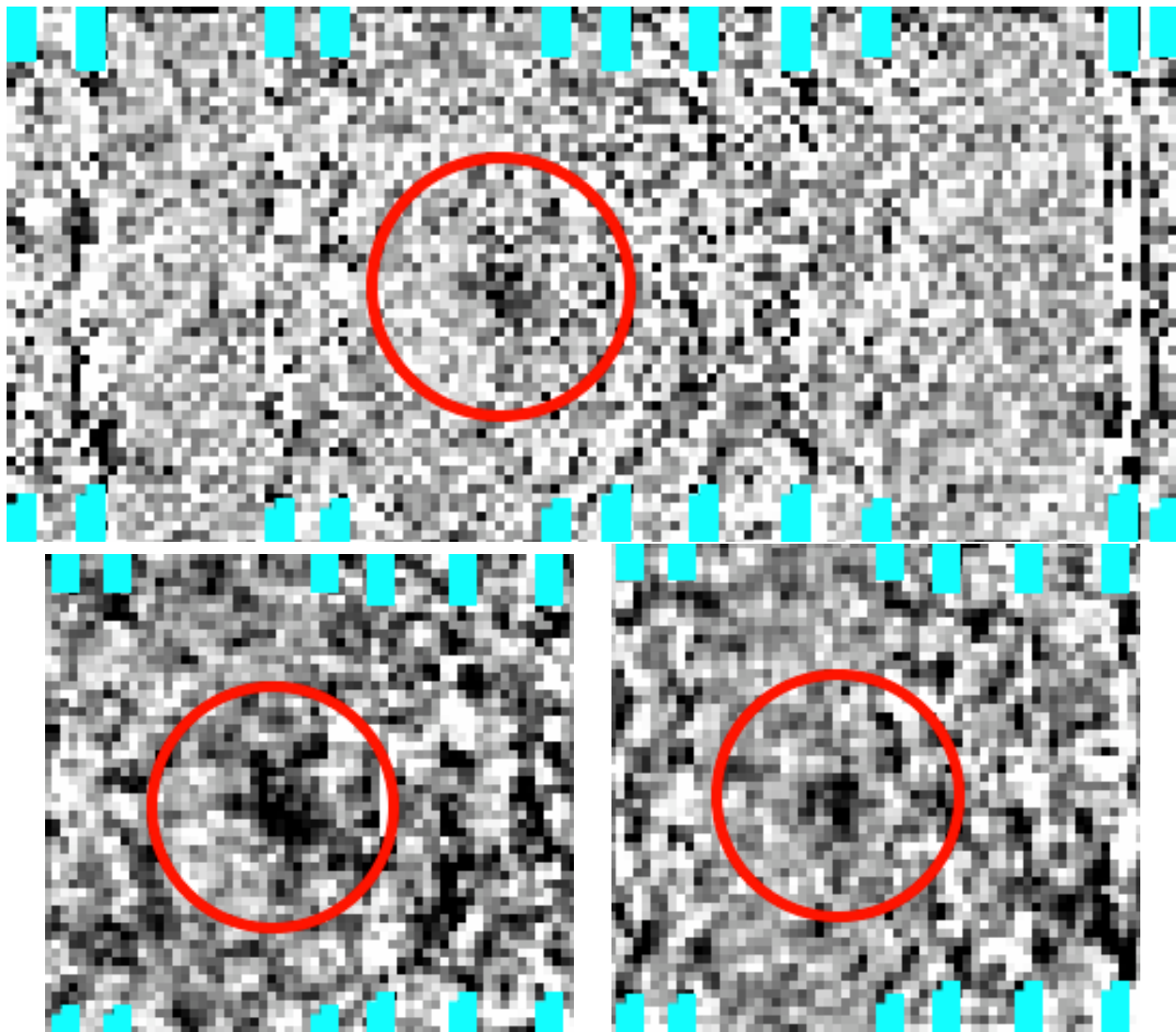


Fig. 1.— 2D spectra of LAE J095950.99+021219.1. *Upper panel:* Full December data set (14 exposures, 7.05 hours' integration) stacked together. Wavelength increases from 9550Å at left to 9800Å at right. The spatial extent is 12'' from bottom to top. *Lower panels:* First night (left) and second night (right) of data separately. The lower panels have been lightly smoothed for clarity, with a Gaussian kernel having $\sigma = 0.6$ pixel. Cyan bars at top and bottom mark the wavelengths of night sky emission lines, with longer bars denoting brighter lines.

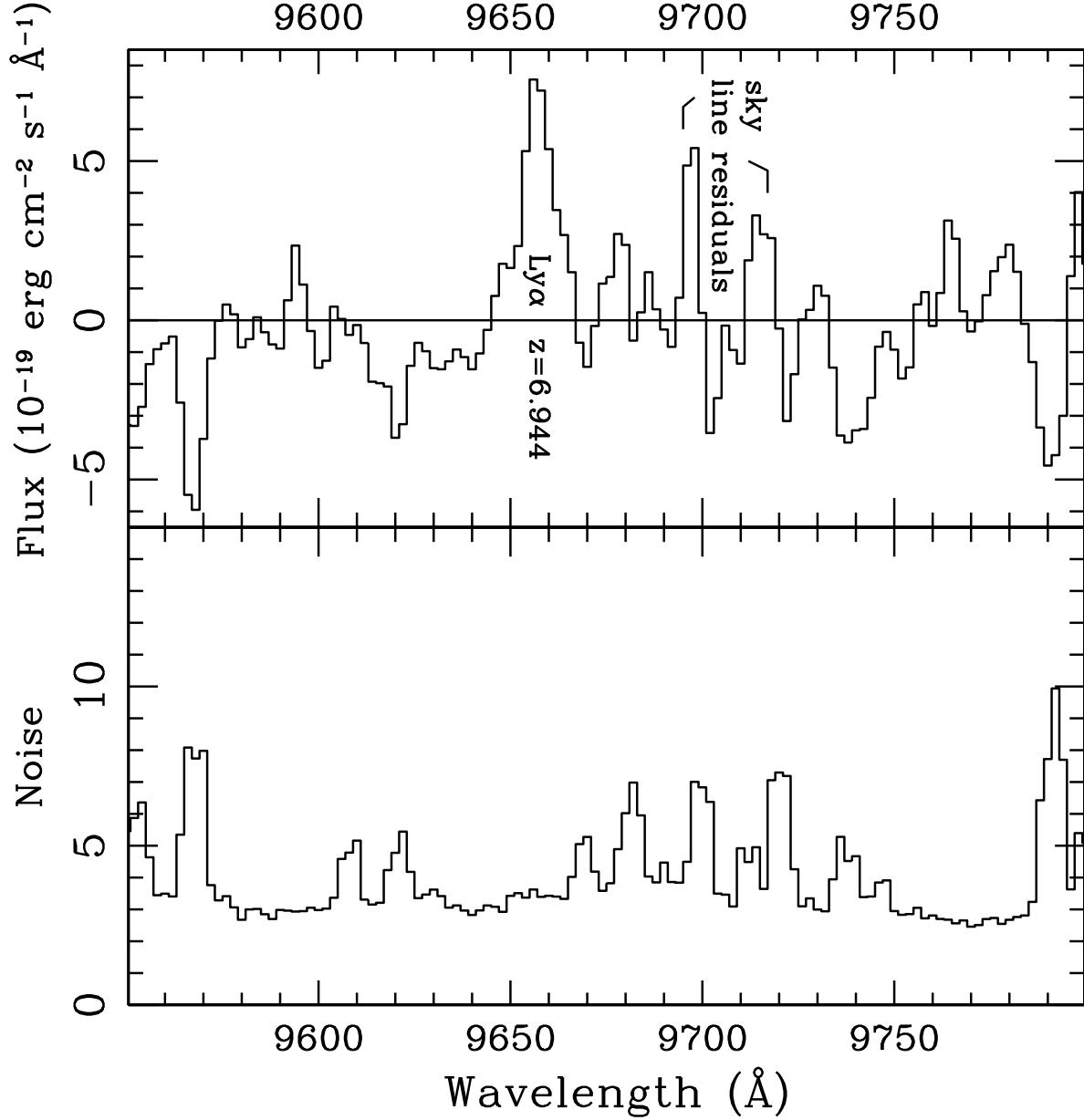


Fig. 2.— The extracted 1D spectrum (lightly smoothed with a “1 2 1” filter, with 4Å FWHM) at top, and a noise estimate (unsmoothed) at bottom. The sole significant feature is the Lyman- α line at 9657Å, corresponding to redshift $z = 6.944$. Some residuals from subtraction of the strong night sky OH emission lines remain, and are marked. The most notable of these is the spike at 9698Å. The plotted noise is based on the sigma image from the 14-frame stack, scaled for the number of spatial pixels combined in the 1D extraction.

If $z = \dots$	Secondary Line	Expected wavelength	Formal flux ($10^{-18} \text{ erg cm}^{-2} \text{ s}^{-1}$)	3σ limit
0.472	[O III] $\lambda 5007$	7370Å	-0.4 ± 1.5	4.1
0.472	[O III] $\lambda 4959$	7299Å	-0.6 ± 0.8	1.8
0.472	H β	7154Å	-0.2 ± 0.8	2.2
0.472	[O II] $\lambda 3727$	5486Å	0.6 ± 1.6	5.4
0.928	[O III] $\lambda 4959$	9565Å	-4.3 ± 4.6	9.5
0.928	H β	9375Å	-12 ± 15	33
0.928	[O II] $\lambda 3727$	7188Å	0.0 ± 0.5	1.5

Table 2: Line flux limits at locations where we would expect emission lines, were the primary line at 9657Å not Lyman- α . $z = 0.472$ corresponds to H α at 9657Å, and $z = 0.928$ corresponds to [O III] $\lambda 5007$ at 9657Å. For comparison, the 9657Å line has flux $8.5 \times 10^{-18} \text{ erg cm}^{-2} \text{ s}^{-1}$. Limits tabulated here are based on fitting a Gaussian line profile to the observed spectrum, with the central wavelength and line width for the fit fixed by the properties of observed line.

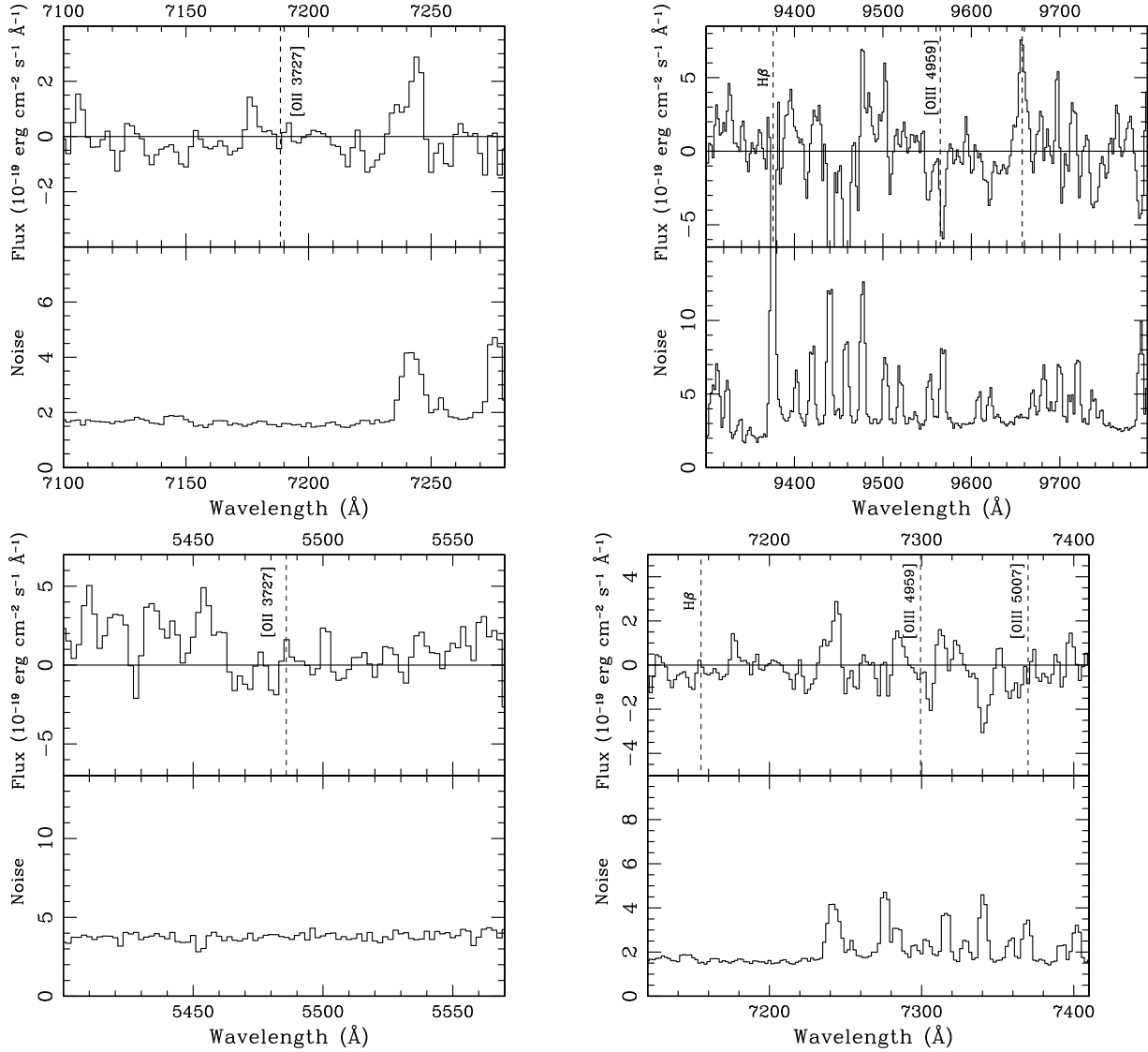


Fig. 3.— If the emission line in LAE J095950.99+021219.1 were not Lyman- α but instead were H α or [O III] λ 5007, we should expect additional emission lines in our optical spectrum. These figures show the expected locations of the [O III] λ 4959,5007, H β , and [O II] λ 3727 lines, for the cases where the primary line is either [O III] λ 5007 at $z = 0.929$ (top two panels) or H α at $z = 0.472$ (bottom two panels). In no case do we see a prominent emission line, although for the $z = 0.929$ case the [O III] λ 4959 and H β lines both fall on night sky line residuals, leaving the absence of an [O II] λ 3727 line at 7188Å and the lack of any optical broad band detection as the best discriminants against this possibility. As in fig. 2, the signal spectra are lightly smoothed with a (1 2 1) filter, while the noise spectra are unsmoothed.